

An Efficient, Single-Source Molecular Precursor to Silicoaluminophosphates

Kyle L. Fuldala and T. Don Tilley*

Department of Chemistry
University of California, Berkeley
Berkeley, California 94720-1460
Chemical Sciences Division
Lawrence Berkeley Laboratory
1 Cyclotron Road, Berkeley, California 94720

Received July 30, 2001

Silicoaluminophosphates¹ (SAPOs) are an important class of solid acids that find wide applications as catalysts and catalyst supports, and considerable current interest centers on their use as catalysts for the conversion of methanol to hydrocarbons.² In general, SAPOs are microporous solids obtained by hydrothermal methods employing organic templates. However, a few reports describe the preparation of mesoporous SAPOs, using aqueous methods and cetyltrimethylammonium salts as templates.³ The relatively complex stoichiometries associated with SAPOs and modified SAPOs, and the sensitivity of their chemical properties to structure,^{1,2b,4} suggest that new synthetic methods could broaden the utility of SAPOs in catalysis.⁵ In this context the development of efficient molecular precursors to SAPOs, containing “pre-formed” O–Si–O–Al–O–P–O linkages, is of interest. In addition, such species might also serve as soluble models for SAPO materials.⁵

We have been investigating the use of single-source molecular precursors of the types $L_nM[\text{OSi}(\text{O}^t\text{Bu})_3]_m$ and $L_nM[\text{OP}(\text{O}(\text{O}^t\text{Bu})_2)]_m$ in nonaqueous transformations to M/Si/O and M/P/O materials with tailored properties.⁶ The goal of the study described here is to develop a single-source molecular precursor for a material with a more complex composition (i.e., Si/Al/P/O), and this work has led to the new heteroelement alkoxide $[(^t\text{BuO})_3\text{SiO}]_2\text{Al}[(\mu\text{-O})_2\text{P}(\text{O}^t\text{Bu})_2]_2\text{Al}(\text{Me})\text{OSi}(\text{O}^t\text{Bu})_3$ (**1**). High surface-area and mesoporous SAPOs have been obtained from **1** via thermolytic molecular precursor routes.⁶

Excess $\text{HOSi}(\text{O}^t\text{Bu})_3$ reacted with $[(\text{Me})_2\text{Al}(\text{O})\text{OP}(\text{O}^t\text{Bu})_2]^{6b}$ (**2**) in toluene at 75 °C to form **1**. Analytically pure crystals were obtained in 62% yield from a mixture of toluene and acetonitrile (10:1) at –30 °C. A single-crystal X-ray structure analysis revealed a molecular structure (Figure 1) featuring distorted tetrahedral geometries for the Si, Al, and P atoms. The average P–O(Al) distance in **1** (1.496(4) Å) is similar to that found for $\text{AlPO}_4\text{-5}$ (1.49 Å) and that calculated for SAPO-5 (1.51 Å).⁷ In

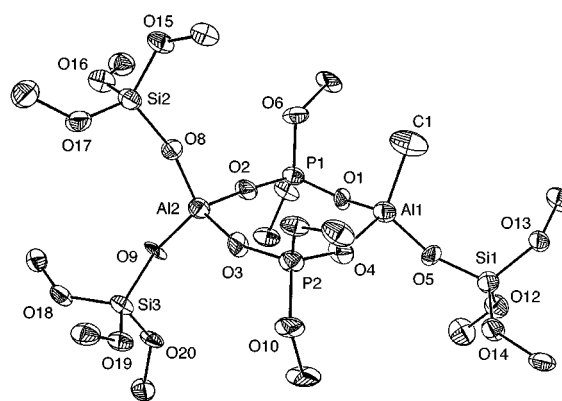
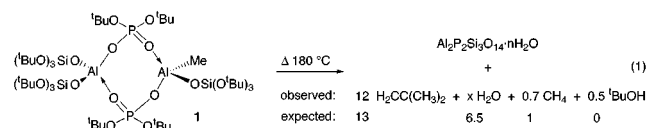


Figure 1. Thermal ellipsoid plot of **1** (50% probability). The ^tBu methyl groups and all hydrogen atoms have been omitted for clarity.

contrast, the average Al–O(P) distance in **1** (1.778(4) Å) is somewhat longer than the corresponding distances in $\text{AlPO}_4\text{-5}$ (1.72 Å) and SAPO-5 (1.71 Å).⁷ The P–O(Al) and Al–O(P) distances in **1** are similar to those in other complexes containing $\text{Al}_2\text{P}_2\text{O}_4$ cores,^{5b,c,d,6b} and the average Al–O(Si) (1.703(4) Å) and Si–O(Al) (1.593(4) Å) distances in **1** are close to those calculated for SAPO-5 (1.67 and 1.55 Å).⁷ The eight-membered $\text{Al}_2\text{P}_2\text{O}_4$ ring structure in **1** is analogous to rings found in some microporous AlPOs and SAPOs.¹

The solid-phase transformation of **1** to a SAPO material was marked by a precipitous mass loss at ca. 150 °C as revealed by thermogravimetric analysis (TGA). This type of behavior signifies an efficient chemical transformation to an oxide material.⁶ Differential scanning calorimetry (DSC) showed that **1** does not melt prior to thermolysis, and no crystallizations were observed up to 1200 °C. The ceramic yield of 32.3% is near that expected for $\text{Al}_2\text{P}_2\text{Si}_3\text{O}_{14}$ (33.2%).⁸

The chemical transformation associated with the conversion of **1** to a SAPO in benzene-*d*₆ produced isobutene, CH₄, and ^tBuOH as the soluble decomposition products (by ¹H NMR spectroscopy, eq 1).⁹ No $\text{HOSi}(\text{O}^t\text{Bu})_3$ or $\text{HOP}(\text{O}(\text{O}^t\text{Bu})_2)$ was detected, suggesting minimal hydrolysis of the Si–O–Al–O–P linkages. No resonances were detected in the ³¹P NMR spectrum after thermolysis, suggesting complete incorporation of the phosphorus from **1** into the SAPO.



A toluene solution of **1** was heated at 180 °C for 24 h to give a clear gel that, upon drying, afforded a xerogel (SAPO_{Xg}). To investigate the use of templates in analogous transformations to mesoporous materials, a toluene solution of **1** was heated at 180 °C for 24 h in the presence of a structure-directing polymer ($\text{EO}_{20}\text{-PO}_{70}\text{EO}_{20}$ or $\text{PO}_{19}\text{EO}_{33}\text{PO}_{19}$, where EO = ethylene oxide and PO = propylene oxide) to yield a xerogel (SAPO_{ep} or SAPO_{pep}) upon drying.¹⁰ Previously, similar copolymers have been em-

(7) Sastre, G.; Lewis, D. W.; Catlow, C. R. *J. Phys. Chem.* **1996**, *100*, 6722.

(8) TGA/DSC analyses were performed using N₂ carrier gas (100 mL min⁻¹) with a heating rate of 10 °C min⁻¹.

(9) The CH₄ is formed from reaction of the Al–Me group with 1 equiv of an “OH” source. The H₂O is not detected due to the SAPO acting as a desiccant. The formation of only a small amount of ^tBuOH also suggests that hydrolysis is not significant during the conversion.

(10) All xerogel samples were calcined at 500 °C in a flow of O₂ to remove residual organic species prior to measurements.

(1) Lok, B. M.; Messina, C. A.; Patton, R. L.; Gajek, R. J.; Cannan, T. R.; Flanigen, E. M. *J. Am. Chem. Soc.* **1984**, *106*, 6092.

(2) (a) Stöcker, M. *Microporous Mesoporous Mater.* **1999**, *29*, 3. (b) Hartman, M.; Kevan, L. *Chem. Rev.* **1999**, *99*, 635.

(3) (a) Chakraborty, B.; Pulikottil, A. C.; Das, S.; Viswanathan, B. *Chem. Commun.* **1997**, 911. (b) Zhao, D.; Luan, Z.; Kevan, L. *Chem. Commun.* **1997**, 1009.

(4) (a) Blackwell, C. S.; Patton, R. L. *J. Phys. Chem.* **1988**, *92*, 3965. (b) Chen, J.; Thomas, J. M.; Wright, P. A.; Townsend, R. P. *Catal. Lett.* **1994**, *28*, 241. (c) Satyanarayana, S. A.; Chilukuri, V. V.; Chakraborty, D. K. *J. Phys. Chem.* **1994**, *98*, 4878.

(5) (a) Murugavel, R.; Prabusankar, G.; Walawalker, M. G. *Inorg. Chem.* **2001**, *40*, 1084. (b) Pinkas, J.; Chakraborty, D.; Yang, Y.; Murugavel, R.; Noltemeyer, M.; Roesky, H. W. *Organometallics* **1999**, *18*, 523. (c) Mason, M. R.; Matthews, R. M.; Mashuta, M. S.; Richardson, J. F. *Inorg. Chem.* **1996**, *35*, 5756. (d) Chakraborty, D.; Horchler, S.; Krätzner, R.; Varkey, S. P.; Pinkas, J.; Roesky, H. W.; Noltemeyer, M.; Schmidt, H.-G. *Inorg. Chem.* **2001**, *40*, 2620. (e) Feher, F. J.; Budzichowski, T. A.; Weller, K. J. *Polyhedron*, **1993**, *12*, 591.

(6) For example: (a) Fuldala, K. L.; Tilley, T. D. *Chem. Mater.* **2001**, *13*, 1817. (b) Lugmair, C. G.; Tilley, T. D.; Rheingold, A. L. *Chem. Mater.* **1999**, *6*, 1615. (c) Terry, K. W.; Lugmair, C. G.; Tilley, T. D. *J. Am. Chem. Soc.* **1997**, *119*, 9745.

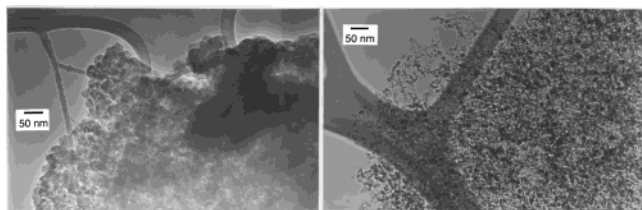


Figure 2. TEM images of SAPO_{xg} (left) and SAPO_{pep} (right).

ployed as structure-directing agents in sol–gel and thermolytic molecular precursor routes to mesostructured materials.¹¹

Low-angle powder X-ray diffraction (PXRD) revealed a single peak in the diffractograms for SAPO_{epe} ($d_{100} = 80 \text{ \AA}$) and SAPO_{pep} ($d_{100} = 115 \text{ \AA}$), indicating a lack of long-range order but suggesting the presence of a disordered hexagonal¹² or wormhole-type pore structure.¹³ No low-angle peak was observed for SAPO_{xg}. High-angle PXRD analyses ($>2\theta = 10^\circ$) revealed no peaks for these xerogels, even after calcination at 1000 °C, indicating that the samples are both homogeneous (atomically well mixed) and thermally stable.^{11c}

Nitrogen porosimetry studies on all of the SAPO materials revealed type IV adsorption–desorption isotherms with hystereses that are intermediate between types H1 and H2.¹⁴ The isotherms for SAPO_{epe} and SAPO_{pep} display a steep rise in adsorption between relative pressures (P/P_0) of 0.6–0.8 with no additional adsorption at $P/P_0 > 0.8$ indicating little textural mesoporosity and suggesting the presence of framework-confined porosity.¹⁵ In contrast to this, the isotherm for SAPO_{xg} exhibits a steep rise in adsorption at $P/P_0 > 0.8$, signifying the presence of substantial textural mesoporosity. The Barrett–Joyner–Halenda (BJH) analyses reveal that SAPO_{epe} and SAPO_{pep} have much narrower pore-size distributions than SAPO_{xg}. The average BJH adsorption (desorption) pore radii were 98 (95), 48 (39), and 33 (33) Å for SAPO_{xg}, SAPO_{epe}, and SAPO_{pep}, respectively.¹⁶ The SAPO materials had high BET surface areas ($>500 \text{ m}^2 \text{ g}^{-1}$) and large pore volumes.¹⁷

Transmission electron microscopy (TEM) revealed that both SAPO_{epe} and SAPO_{pep} consist of similarly sized particles, whereas SAPO_{xg} possesses a wide distribution of larger particles (Figure 2). The similar size of the particles within SAPO_{epe} and SAPO_{pep} accounts for their narrow pore-size distributions, suggesting that the polymer “templates” behave only as anisotropic space fillers on co-thermolysis with **1**. The structures of SAPO_{epe} and SAPO_{pep} appear to be more open and fibrous than that of SAPO_{xg}. Energy-dispersive X-ray spectroscopy (EDX), performed on multiple areas of each xerogel, revealed that the Al/Si/P ratios ranged from 2:3:1:1.7 to 2:4.0:2.1 ($\pm 10\%$), indicating that the stoichiometry of **1** is maintained on thermolysis.

(11) (a) Prouzet, E.; Pinnavaia, T. J. *Angew. Chem., Int. Ed. Engl.* **1997**, *36*, 516 and references therein. (b) Zhao, D. Y.; Feng, J. L.; Huo, Q. S.; Melosh, N.; Fredrickson, G. H.; Chmelka, B. F.; Stucky, G. D. *Science* **1998**, *279*, 548 and references therein. (c) Kriesel, J. W.; Sander, M. S.; Tilley, T. D. *Adv. Mater.* **2001**, *13*, 331.

(12) Bagshaw, S. A.; Prouzet, E.; Pinnavaia, T. J. *Science*, **1997**, *277*, 552.

(13) Pauly, T. R.; Liu, Y.; Pinnavaia, T. J.; Billinge, S. J. L.; Rieker, T. P. *J. Am. Chem. Soc.* **1999**, *121*, 8835.

(14) Gregg, S. J.; Sing, S. W. *Adsorption, Surface Area, and Porosity*, 2nd ed.; Academic Press: London, 1982.

(15) Tanev, P. T.; Pinnavaia, T. J. *Chem. Mater.* **1996**, *8*, 206.

(16) Average pore radii as calculated using “2(pore volume)/area”: SAPO_{xg} 66 Å; SAPO_{epe} 40 Å; SAPO_{pep} 33 Å.

(17) Surface areas and pore volumes ($\text{m}^2 \text{ g}^{-1}$, $\text{cm}^3 \text{ g}^{-1}$): SAPO_{xg} 510, 1.68; SAPO_{epe} 570, 1.14; SAPO_{pep} 510, 0.84.

Table 1. Acidic Properties of the Materials from **1** and of SBA-15.

	total acid sites	OH sites	Lewis sites
SAPO _{xg}	$5.3 \pm 0.2 \text{ nm}^{-2}$	$2.0 \pm 0.2 \text{ nm}^{-2}$	$3.3 \pm 0.3 \text{ nm}^{-2}$
SAPO _{epe}	$4.7 \pm 0.3 \text{ nm}^{-2}$	$1.3 \pm 0.1 \text{ nm}^{-2}$	$3.4 \pm 0.3 \text{ nm}^{-2}$
SAPO _{pep}	$4.9 \pm 0.4 \text{ nm}^{-2}$	$1.4 \pm 0.1 \text{ nm}^{-2}$	$3.5 \pm 0.4 \text{ nm}^{-2}$
SBA-15	$1.0 \pm 0.1 \text{ nm}^{-2}$	$1.0 \pm 0.1 \text{ nm}^{-2}$	N/A

The ²⁷Al and ³¹P MAS NMR spectra of SAPO_{xg} exhibited one broad resonance centered at 33.2 and -26.9 ppm , respectively. Such resonances are indicative of tetrahedrally coordinated Al and P in AlPOs and SAPOs.^{4a,18} The broadness of the ²⁷Al resonance suggests the presence of more than one Al(OP)_x(OSi)_y environment.¹⁸

The temperature-programmed desorption (TPD) of ammonia (monitored by TGA) was used to determine the total concentration of acid sites for the xerogels. Reaction with Mg(CH₂Ph)₂·2THF was used to quantify the concentration of OH sites by determining the amount of toluene produced (monitored by ¹H NMR spectroscopy). For comparison, identical measurements were made for the mesoporous silica material SBA-15^{11b} (calcined at 500 °C). Acidity data are summarized in Table 1. It appears that the SAPOs synthesized here contain mostly weak Brønsted acid sites, as evident by a maximum rate of NH₃ desorption occurring below 150 °C. Despite this, loss of NH₃ was evident at temperatures $>200 \text{ °C}$, suggesting the presence of some stronger sites.

Infrared spectra of the SAPO xerogels all contained several broad overlapping stretches from ca. 3180 to 3700 cm^{-1} in the ν_{OH} region. For example, the IR spectrum of SAPO_{xg} displayed peaks at 3698, 3647, 3628, 3607, 3391, and 3180, cm^{-1} , revealing several different hydroxyl groups. Infrared stretches from 3500 to 3800 cm^{-1} have been attributed to various types of bridging and terminal P–OH, Al–OH, and Si–OH groups in microporous SAPOs.¹⁹

In summary, a new heteroelement alkoxide based on Si, Al, and P was synthesized and used as a single-source molecular precursor to high Si content, thermally stable, high surface area, and mesoporous SAPO xerogels. The physical properties of SAPO_{xg}, SAPO_{epe}, and SAPO_{pep} indicate that they could be excellent catalysts and support materials, especially for reactions involving large organic substrates. To that end, we are currently investigating their catalytic properties. Finally, complex **1** is a soluble model for SAPOs due to its novel O–Si–O–Al–O–P–O–Al–O–Si–O chain of atoms.

Acknowledgment. This work was supported by the Director, Office of Energy Research, Office of Basic Energy Sciences, Chemical Sciences Division, of the U.S. Department of Energy under Contract No. DE-AC03-76SF00098. We thank E. C. Nelson at the National Center for Electron Microscopy for assistance with the EDX analyses and B. L. Phillips at UC Davis for the MAS NMR spectra.

Supporting Information Available: Experimental details, TGA, PXRD, N₂ porosimetry, TEM, IR, MAS NMR, and crystallographic data (PDF). An X-ray crystallographic file (CIF). This material is available free of charge via the Internet at <http://pubs.acs.org>.

JA0167295

(18) (a) Ojo, A. F.; Dwyer, J.; Dewing, J.; O’Malley, P. J.; Nabhan, A. J. *Chem. Soc., Faraday Trans.* **1992**, *88*, 105. (b) Chakraborty, B.; Pulikottil, A. C.; Viswanathan, B. *Appl. Catal., A* **1998**, *167*, 173. (c) Luan, Z.; Zhao, D.; He, H.; Klinowski, J.; Kevan, L. *J. Phys. Chem. B* **1998**, *102*, 1250.

(19) Chen, J.; Wright, P. A.; Thomas, J. M.; Natarajan, S.; Marchese, L.; Bradley, S. M.; Sankar, G. S.; Catlow, C. R. A. *J. Phys. Chem.* **1994**, *98*, 10216 and references therein.